HIGH VOLTAGE INSULATOR CONTAMINATION LEVEL MONITORING WITH X-BAND MICROWAVE RADIOMETER

Yan JIANG, Alistair REID, Azam NEKAHI, Scott G MCMEEKIN
Glasgow Caledonian University-UK
yan.jiang@gcu.ac.uk

Martin JUDD
HFDE Ltd-UK
m.judd@hfde.co.uk

Alan WILSON
Doble PowerTest Ltd-UK
AWilson@doble.com

ABSTRACT

This paper introduces a novel method for monitoring contamination levels on high voltage insulators based on microwave radiometry. The microwave radiometer described measures energy emitted from the contamination layer and could provide a safe, reliable, contactless monitoring method that is effective under dry conditions. The relationship between equivalent salt deposit density and radiometer output is described using a theoretical model and experimentally verified using a specially designed X-band radiometer. Results demonstrate that the output from the radiometer is able to clearly distinguish between samples with different contamination levels under dry conditions. This novel contamination monitoring method could potentially provide advance warning of the future failure of wet insulators in climates where insulators can experience dry conditions for extended periods.

1. INTRODUCTION

High Voltage insulators are employed extensively in overhead transmission lines and substations and form an essential component in power systems and networks. The build-up of surface contamination on the insulators can lead to an increase in leakage current and partial discharge which may eventually result in flashover. Most commercial contamination monitoring systems are based on leakage current measurements using either a current transformer or a shunt resistor with an electrode ring to intercept the leakage current. Such systems suffer from two drawbacks: (1) their physical installation onto insulator circuit would reduce insulation security, and (2) systems are only effective when the contamination layer has been wetted by rain, fog or condensation; under this condition flashover is likely to occur within a short time period [1].

In order to address these problems, this paper presents a novel monitoring method based on microwave radiometry. Microwave radiometry is one of the basic techniques for measuring electromagnetic radiation and has been widely used in astronomy, meteorology, oceanography, geography and hydrology [2]. Electromagnetic radiation of a material will cover a very wide frequency band. The distribution of the spectrum is a function of material's emissivity and temperature. The emissivity ε of a material represents the relative ability of its surface to emit energy by radiation and is referred to as the brightness temperature T_B. Brightness temperature (BT) refers to the temperature of a blackbody that would radiate the same power [3]. A polluted insulator emits a different electromagnetic energy level compared to a clean insulator due to the contamination layer. Thus, a radiometer, or passive receiver that detects the input power in a specific frequency band using an antenna, has the ability to monitor pollution level on an insulator surface.

In the present paper a theoretical model is developed based on remote sensing techniques which in turn were developed for soil salinity detection. An X-band (8.0 to 12.0 GHz) radiometer with high sensitivity and stability with relatively low cost was designed especially for monitoring insulator surface. A laboratory experiment was implemented to verify the consistency between theoretical model and practical radiometer outputs under dry condition. The results show the potential and feasibility of applying this novel monitoring method to enable advanced warning on high polluted insulators.

2. THEORETICAL MODEL

Radiometers are widely used in remote sensing for soil moisture distribution and work has been published on models to provide the soil salinity from brightness temperature [4]. Brightness temperature is affected by several unknown parameters including moisture, salinity, bulk density, thickness and surface roughness. Obtaining Equivalent Salt Deposit Density (ESDD) on insulator might therefore be treatable in a similar manner to soil salinity detection problems. For a contamination layer on an insulator, the influence of thickness and surface roughness can be ignored when compared to moisture and salinity because the layer is relativity thin with a smooth surface. The bulk density is calculated based on the properties of the artificial contamination layer described in IEC standard 60507. Thus, the key parameters that need to be inferred are moisture and salinity.

Figure 1 shows the structure of the proposed system model relating radiometer output to ESDD. Within this framework, the dielectric mixing model evaluates the dielectric properties of insulator contamination layer as a function of moisture, salinity, environment temperature and humidity by assuming it as salt and water affected soil. The brightness temperature model describes the relationship between dielectric properties, emissivity and

brightness temperature of a contaminated insulator. Finally, the radiometer model converts input power to output voltage and is related to system design.

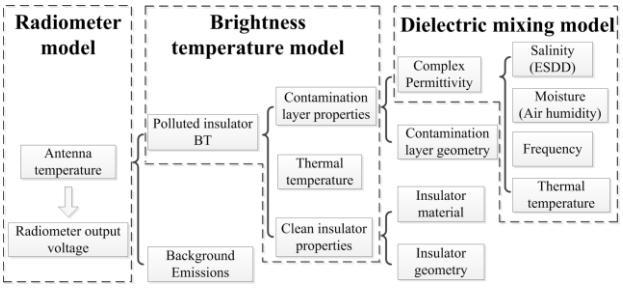

Figure 1. Theoretical model of applying radiometry to monitor insulator contamination.

2.1 Dielectric mixing model

The dielectric mixing model developed by Dobson [5] is a classical model for remotely sensing soil moisture. It gives the dielectric constant of soil as a function of its water content. In consideration of the effect of the salt on the soil, the dielectric mixing model needs to be modified as this model only works under very low salt content. After replacing water's dielectric constant model in the dielectric mixing model by the dielectric constant model of saline water which was developed by Stogryn [6], the dielectric mixing model will carry the information of both soil moisture and soil salinity. On the insulator surface, moisture is a function of air humidity which can be easily measured.

Lane and Saxton modified a Debye-type relaxation to account for ionic-conductivity losses caused by salinity of the water [7]. In terms of Stogryn's formulation, the real and imaginary parts of the dielectric constant of saline water are respectively given by [4]:

$$\begin{cases} \varepsilon'_{sw} = \varepsilon_{sw\infty} + \frac{\varepsilon_{sw0}-\varepsilon_{sw\infty}}{1+(2\pi f\tau_{sw})^2} \\ \varepsilon''_{sw} = \frac{2\pi f\tau_{sw}(\varepsilon_{sw0}-\varepsilon_{sw\infty})}{1+(2\pi f\tau_{sw})^2} + \frac{\sigma_{NaCl}}{2\pi\varepsilon_0 f} \end{cases} \quad (1)$$

where $\varepsilon_{sw\infty} = \varepsilon_{w\infty} = 4.9$ and $\varepsilon_0 = 8.854 \times 10^{-12}(F/m)$ is the permittivity of free space.

Dobson's model of Equation (2) below, represents the dielectric constant of soil is a function of soil moisture m_v, dielectric constant of free water inside soil ε_{fw}, permittivity of dry soil ε_s, bulk density of dry soil ρ_s and bulk density of wet soil ρ_b.

$$\begin{cases} \varepsilon'_m = (1 + (\rho_b/\rho_s)\varepsilon_s^{\alpha} + m_v^{\beta'}\varepsilon_{fw}'^{\alpha} - m_v)^{\frac{1}{\alpha}} \\ \varepsilon''_m = (m_v^{\beta''} \cdot \varepsilon_{fw}''^{\alpha})^{\frac{1}{\alpha}} \end{cases} \quad (2)$$

where, α and β are related to the soil texture. By combining equation (2) with Stogryn's model, free water is considered as saline water where: $\varepsilon'_{fw} = \varepsilon'_{sw}$ and $\varepsilon''_{fw} = \varepsilon''_{sw}$. In IEC standard 60507, the contamination layer is entirely consisting of Kaolin, which is a form of clay. The typical bulk density of clay is ρ_b=1g/cm^3.

2.2 Brightness temperature model

An insulator's radiance can be expressed in terms of its brightness temperature:

$$T_B = \varepsilon T_o = (1 - R)T_o \quad (3)$$

where R is the Fresnel reflection coefficient on the insulator surface and *To* is the temperature in Kelvin of the contaminated insulator. A brightness temperature model is applied to transform the geometry structure of the insulator and dielectric properties to emissivity and finally the brightness temperature of the contaminated insulator.

In a practical environment, the insulator is in air and is contaminated on the surface. The surrounding air forms a third layer. We assume that the insulator surface with contamination is a double-layer homogeneous dielectric plate with a smooth surface, as shown in Figure 2. Thus, a double layer model is applied to calculate the brightness temperature of the contaminated insulator. The reflection coefficient of this double layer is given by [8]:

$$R = \frac{R_{01}+R'_{12}exp(-j2\delta_1)}{R_{01}R'_{12}exp(-j2\delta_1)+1} \quad (4)$$

Where

$$R'_{12} = \frac{R_{12}+R_{23}exp(-j2\delta_2)}{R_{12}R_{23}exp(-j2\delta_2)+1} \quad (5)$$

And

$$\delta_i = \frac{2\pi d_i}{\lambda}\sqrt{\varepsilon_i^2 - sin^2\theta} \quad (6)$$

Where λ is the wavelength in free space, ε_i is the complex permittivity of the *i*-th layer, d_i is the thickness of the *i*-th layer and θ is the angle of incidence. R_{12} is Fresnel's reflection coefficient for the interface between the air and the contamination layer. R_{23} is the reflection coefficient for the interface between the contamination layer and the insulator. Note that the values of R_{12} and R_{23} are polarization sensitive.

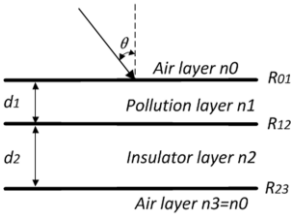

Figure 2. Double dielectric layer model of contaminated insulator surface.

2.3 Discussion

To demonstrate the model predictions for a simple geometry, Figure 3 presents the relationship between salinity, frequency, moisture, angle of incidence and brightness temperature of a contaminated flat glass plane. The brightness temperature increases with the increasing of the salinity of the contamination layer at 0 ° angle of incidence as shown in Figure 3(a). The gradients of brightness temperature curves are higher at high moisture

levels. Therefore, the radiometer has a better sensitivity to detect the ESDD of contaminated insulator under wet condition than dry condition. According to Figure 3(b), the system has a higher sensitivity to the contamination level at lower frequencies. Two protected frequency bands at 1.4 GHz and 10.6 GHz are always chosen for radiometer system operation to avoid interference from radar and communication system [9]. The dielectric constant is much more sensitive to the water content and salinity at 1.4 GHz, a typical frequency band used for soil moisture and sea water salinity sensors on satellites [4]. However, the wavelength at 1.4 GHz is 214.2 mm, which is too large to provide a reasonable spatial resolution in relation to size of the insulators under test. X-band (10.6 GHz, λ=28.3mm) was therefore chosen to achieve a balance between system sensitivity and spatial resolution.

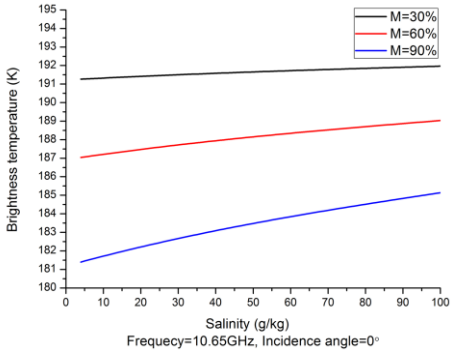

(a)

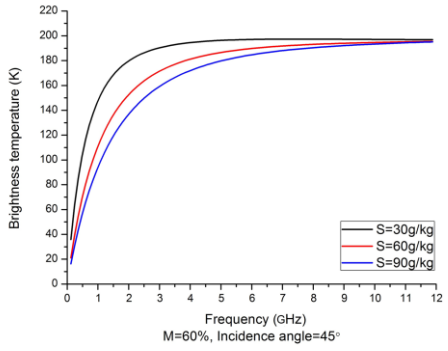

(b)

Figure 3. Theoretical relationship between Brightness temperatures and (a) salinity at different moisture level, (b) frequency at different salinity levels.

3. RADIOMETER SYSTEM

3.1 Radiometer design

The radiometer system developed for monitoring pollution levels on insulators is based on a Dicke radiometer with a superheterodyne architecture, as shown in Figure 4. The radiometer system can be divided into five sections: (1) RF Input, (2) front-end, (3) downconverter, (4) back-end and (5) data acquisition (DAQ). The RF input signal to the radiometer systems is captured using a horn antenna with 20 dB gain, pointed towards to insulator sample. The system used in these experiments is a passive receiver with the centre frequency of 10.65 GHz and 1 GHz bandwidth. A superheterodyne circuit downcoverts the 10.65 GHz signal to 0 - 500 MHz before a digital lock-in amplifier provides a dc output voltage that is linearly proportional to the input power at the antenna. The design of the system has focused on optimizing accuracy, stability and sensitivity using a relatively low cost architecture.

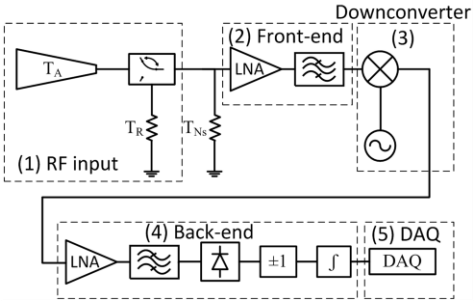

Figure 4. Block diagram of the X-band Dicke radiometer.

The classical Dicke radiometer, shown in Figure 4, uses a radio frequency (RF) switch to allow continuous comparison between the input power and an internal reference. The output of this Dicke radiometer can be expressed as [2]:

$$V_{out} = c(T_A + T_{Ns})G - c(T_R + T_{Ns})G = c(T_A - T_R)G \quad (7)$$

where c is a constant, G is the system gain, T_R is the equivalent antenna temperature of the internal reference signal and T_{Ns} is the system noise temperature generated by the thermal noise and instabilities of the individual components in the radiometer system. T_A is the antenna temperature which relates to the brightness temperature of the sample and background radiation and can be expressed as:

$$T_A = T_{AP} + T_{NPE} \quad (8)$$

where T_{AP} is the antenna temperature generated by the polluted test sample and T_{NPE} represents the contribution to the antenna temperature due to the background radiation of the surrounding environment of the test sample.

During initial testing of the Dicke radiometer on the insulator samples, the system was found to be very sensitive to external environmental conditions, such as changes in ambient temperature, background lighting and external RF interference. To address this issue an external reference signal from an antenna pointed at a clean sample was used to replace the internal thermal reference used in the classical Dicke radiometer system. Thus, T_R in Equation (7) can be replaced by:

$$T_R = T_{AC} + T_{NCE} \quad (9)$$

where T_{AC} is the antenna temperature generated by the clean reference sample and T_{NCE} is the antenna temperature generated by the background radiation of the reference sample. It was important to minimize any difference in the positioning of the samples relative to the

antenna to ensure that both have same experimental conditions, such as surface temperature and background RF interference.

By replacing the internal reference of the classic Dicke radiometer with an external reference, the antenna equation (7) is modified to:

$$V_{out} = c(T_{AP} + T_{Ns} + T_{NPE})G - c(T_{AC} + T_{Ns} + T_{NCE})G$$
$$= c(T_{AP} - T_{AC})G + c(T_{NPE} - T_{NCE})G \quad (10)$$

Since the polluted and clean samples have similar surrounding environmental conditions, these components will cancel out allowing Equation (10) to be expressed as:

$$V_{out} = c(T_{AP} - T_{AC})G \quad (11)$$

The system output becomes dependent only on the brightness temperature differences between the polluted and clean insulator. The difference in the brightness temperature can be correlated to a change in ESDD levels.

3.2 Calibration

The calibration of a conventional Dicke radiometer uses two RF terminations with different, well-known noise temperatures to replace the antenna at the radiometer input. The relationship between antenna temperature and output voltage can be found from two data sets according to Equation (11). In our system, the external reference does not have a constant noise temperature compared to an internal reference. Thus, the system output voltages of two clean samples with the same material and geometry as the external reference but at different thermal temperatures are recorded to give the system equation:

$$V_{diff} = V_{offset} + 0.1021 \cdot T_{diff} \quad (12)$$

where V_{diff} is the output voltage after lock-in amplifier, V_{offset} = 21.0 mV is the calculated internal voltage difference brought by RF switch and T_{diff} is the antenna temperature difference between sample and reference.

4. EXPERIMENT

4.1 Samples

To remove the effect of complex surface geometry of the HV insulators for the purpose of testing the concept, it was decided to use flat glass planes for the initial evaluation tests. The glass plane is 500 x 200 mm and 8 mm thick. The solid layer method recommended by IEC standard 60507 was employed to form an artificial pollution layer on the sample surfaces. This method involves uniformly spraying a pollution suspension on the sample surfaces to form a solid layer. The composition of the suspension used in tests comprised 6.5 g Kaolin, 150 g water and a suitable amount of NaCl to control the ESDD level. A 150 ml suspension was sprayed evenly on one sample surface and the sample was then left to dry for 48 hours in a low humidity room. After the tests had been completed, the solid layers were washed off with 500 ml distilled water and the ESDD of each sample was obtained by measuring the conductivity of the washing water and then calculated using Equation (10):

$$\begin{cases} ESDD = S_a \cdot V/A \\ S_a = (5.7 \cdot \sigma_{20})^{1.03} \end{cases} \quad (13)$$

where S_a is the salinity, σ_{20} is the conductivity of the NaCl solution corrected to 20 ℃, V is the volume of distilled water and A is the sample surface area.

Four glass samples with 4 different contamination levels were tested. Table 1 lists the properties of the contamination layers on these sample pairs.

Table 1. The properties of the contamination layers on 4 sample pairs.

Sample	NaCl (g)	ESDD on glass (mg/cm^2)
1	3	0.0236
2	9	0.0641
3	15	0.1027
4	18	0.1176

4.2 Experimental setup

The radiometer was allowed to stabilize for 1 hour before each test to achieve thermal stability within the system. Each sample was measured 40 times to remove errors generated by the impulsive noise lasting shorter than the switching time and to study the repeatability of the experiment. For each measurement, the radiometer outputs from the lock-in amplifier were recorded to provide a single dc value which is proportional to the average brightness temperature difference between the sample and the reference within 20 s time period.

4.3 Results

Figure 5 shows a typical original output voltage before the digital lock-in amplifier during the 20 s integration time. The output voltages of the sample and the reference presented are clearly different by about 30 mV and the value would be further extracted by the lock-in amplifier. White noise on the output signal can be attributed to the thermal noise of the components in radiometer system. The transient noises were most likely generated by either switching or external RF interference.

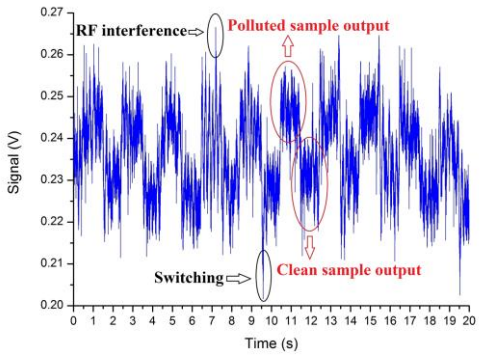

Figure 5. Output voltage of radiometer before the digital lock-in amplifier.

In order to verify the agreements between the experimental results and the theoretical model, the theoretical brightness temperature was calculated based on Equations (1-6) by using the particular parameters from the experiment and then converted to radiometer output voltages based on Equation (12). Figure 6 show the validation of the theoretical model by experimental results under dry condition of the glass samples.

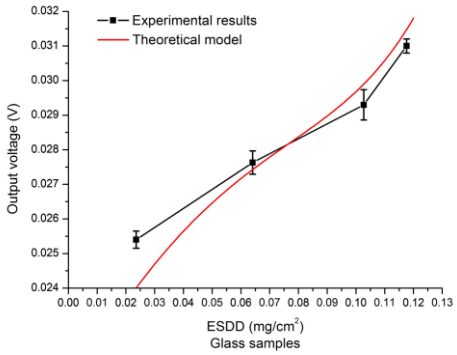

Figure 6. Output voltage from microwave radiometer system and theoretical model as a function of ESDD levels.

Figure 6 indicates good agreement between the theoretical model and the experimental results for the output voltage from the microwave radiometer system as a function of ESDD levels on a glass substrate. The results show that the radiometer output voltage increases with the increasing of the ESDD levels on a glass sample's surface. The error bars of experimental results show the range of values obtained across 40 repeat measurements taken for each sample. The disagreement of the first sample may be attributed to the variations in contamination level due to the particularly low concentration of NaCl in this case.

5. CONCLUSION

This paper has described a study into the feasibility of using an X-band radiometer to assess the contamination level on HV insulators both by theory and experiment. The theoretical model developed the relationship between the contamination layer, ESDD levels, dielectric properties and brightness temperature. Experimental work involved a novel implementation of an improved Dicke radiometer and demonstrated good agreement with theoretical predictions. This work provides a foundation for future investigations into the development of an on-line monitoring system for insulator pollution that is effective under dry conditions.

In future, the effect of complex surface geometry of insulator and Non-Soluble Salt Deposit Density (NSDD) will be studied. Because this novel method suffers very high external noise from surrounding environments, further de-noising technology will be necessary for onsite testing.

Acknowledgments

The authors would like to thank Doble Powertest and the Energy Technology Partnership (ETP) for funding this project.

REFERENCES

[1] S. M. Gubanski, A. Dernfalk, J. Andersson, and H. Hillborg, 2007, "Diagnostic Methods for Outdoor Polymeric Insulators," *Dielectrics and Electrical Insulation, IEEE Transactions on*, vol. 14, pp. 1065-1080..

[2] N. Skou and D. M. L. Vine, 2006, *Microwave Radiometer Systems: Design and Analysis*: Artech House, UK

[3] M. Z. Rahman, L. Roytman, and A. H. Kadik, 2013, "Refining environmental satellite data using a statistical approach", *Proc. SPIE 8723, Sensing Technologies for Global Health, Military Medicine, and Environmental Monitoring III*, Baltimore, Maryland, USA."

[4] Y. Lasne, P. Paillou, A. Freeman, T. Farr, K. C. McDonald, G. Ruffie, *et al.*, 2008, "Effect of Salinity on the Dielectric Properties of Geological Materials: Implication for Soil Moisture Detection by Means of Radar Remote Sensing", *Geoscience and Remote Sensing, IEEE Transactions on*, vol. 46, pp. 1674-1688.

[5] M. C. Dobson, F. T. Ulaby, M. T. Hallikainen, and M. A. El-Rayes, 1985, "Microwave Dielectric Behavior of Wet Soil-Part II: Dielectric Mixing Models", *Geoscience and Remote Sensing, IEEE Transactions on*, vol. GE-23, pp. 35-46.

[6] A. Stogryn, 1971, "Equations for Calculating the Dielectric Constant of Saline Water", *Microwave Theory and Techniques, IEEE Transactions on*, vol. 19, pp. 733-736.

[7] J. A. Lane and J. A. Saxton, 1952, "Dielectric Dispersion in Pure Polar Liquids at Very High Radio Frequencies. III", *The Effect of Electrolytes in Solution* vol. 214.

[8] K. Sato, H. Kozima, H. Masuzawa, T. Manabe, T. Ihara, Y. Kasashima, *et al.*, 1995, "Measurements of reflection characteristics and refractive indices of interior construction materials in millimeter-wave bands", *IEEE 45th Vehicular Technology Conference*, vol.1, pp. 449-453.

[9] E. C. Committee, 2013, "The european table of frequency allocations and applications in the frequency range 8.3 kHz to 3000 GHz", *European Conference of Postal and Telecommunications Administrations*.